International Journal of Heat and Mass Transfer 52 (2009) 1245–1253

Contents lists available at ScienceDirect

International Journal of Heat and Mass Transfer

journal homepage: www.elsevier.com/locate/ijhmt

Freezing on subcooled surfaces, phenomena, modeling and applications

Frank G.F. Qin [a,*], Xiao Dong Chen [b], Kevin Free [a]

[a] Freezecon Limited, Department of Chemical and Materials Engineering, The University of Auckland, Private Bag 92019, Auckland, New Zealand
[b] Department of Chemical Engineering, Monash University, Building 36, Clayton Campus, Vic. 3800, Melbourne, Australia

ARTICLE INFO

Article history:
Received 20 December 2007
Received in revised form 28 June 2008
Available online 1 November 2008

Keywords:
Ice fouling
Thermal response
Growth kinetics
Ice
Freeze concentration
Modelling

ABSTRACT

At the onset of ice nucleation from aqueous solutions on a subcooled solid surface, experiments show that the heat flux across the cooling surface has a steep increase. If scraping action is applied to prevent ice fouling on the cooling surface, high-level heat transfer will continue. In this paper, the following subjects are studied: (1) the time required for ice to cover the unscraped cooling surface; (2) the thermal response of the supercooled solution at the onset of phase change; (3) the heat transfer coefficient on the scraped surface with/without phase change, and (4) the growth kinetics of ice film spreading along the cooling surface. The outcome is applied to improve the design and operation of the scraped surface heat exchange, which is used to produce ice slurry in freeze concentration, desalination or cold storage.

1. Introduction

1.1. History

The earliest scientific study of the growth of ice layer on a subcooled surface began in the field of geography by Lame, Clapyron, and Neumann et al. in the middle of the nineteenth century. Phenomenon observation and mathematical analysis generated the famous Neumann problem of the partial differential equations, which greatly contributed to the early establishment of modern heat and mass transfer theory. A typical form of the Neumann Problem is expressed as the following simultaneous equations and illustration in Fig. 1 [1].

Symbol explanations are shown in the Nomenclature. In the Neumann problem, the beginning of the phase change of water is assumed to be uniform all over the subcooled surface, i.e. ice appears as a thin film, which then thickens evenly in the perpendicular direction.

At the onset of freezing on a subcooled surface, we understand nowadays that primary nucleation will not occur uniformly and simultaneously at every inch of the surface, but at some spots where there exist microscopic defects in the material. The physical interpretation of the Neumann problem for the heat and mass transfer and the mathematical treatment of the problem proved to be significant and meaningful in a wide range of science and engineering fields. The importance of the classical Neumann Problem is not in the treatment and interpretation for the onset of phase change (nucleation), but the subsequent process of the unsteady heat and mass transfer.

However, the heat and mass transfer at the onset of phase change is still an important subject, e.g. freezing on the subcooled surfaces is of great interest for a variety of scientific and engineering applications, such as the formation of a multi-molecule layer of ice on a single crystalline surface [2]; the condensing and the ice films formation on the superconducting magnet for confining and managing plasma bunch in the next generation of fusion devices [3,4]; and the scraped surface heat exchanger (SSHE) used for making ice slurry for freeze concentration [5–7], wastewater treatment [8–11], desalination and cold storage in energy industry, etc. [12,13]. It is attracting growing attention nowadays because fresh water and/or energy shortage are becoming a critical problem in more and more places world-wide. Though the industrial practice of using SSHE to produce ice slurry can be dated back to the 1970s, more details regarding the optimal scraping tension and frequency to improve the efficiency are needed [14–17].

1.2. Experimental background of current study

Previous publications of this work [18,19] regarding the microscopic observation of the onset of ice formation described the phenomenon that ice actually appeared in a number of spots on the subcooled surface. They spread in transversal directions along the surface to form ice films, during this time the thickness of the ice film hardly changing until the cooling surface was fully covered. Figs. 2 and 3 are some frames from two video clips of the

* Corresponding author. Tel.: +64 9 3737599x86293; fax: +64 9 3737463.
E-mail address: f.qin@auckland.ac.nz (F.G.F. Qin).

0017-9310/$ - see front matter © 2008 Elsevier Ltd. All rights reserved.
doi:10.1016/j.ijheatmasstransfer.2008.09.010

Nomenclature

A_s cooling surface area (m^2)
C_{seed} mass fraction of ice seed added to start the ice crystallization in the undercooled solution
c_l, c_w specific heat capacity of the liquid (= 3910 for 10%wt sucrose solution) and solid wall (=502.3 for stainless steel) respectively (J kg^{-1} °C^{-1})
F number of blades of the rotational scraper, each of them wipes over the entire cooling surface once every revolution
h individual heat transfer coefficient on the cooling surface (W m^{-2} °C^{-1})
ΔH latent heat of water freezing (=334) (kJ kg^{-1})
I_0 modified Bessel functions of the first kind of the zero order
I_1 modified Bessel functions of the first kind of the first order
K_0 modified Bessel functions of the second kind of the zero order
K_1 modified Bessel Functions of the second kind of the first order
k_{il} rate constant of ice formation in liquid (bulk), which is defined as the ice production rate per cubic meter of solution per degree of supercooling (=0.384 for 10%wt sucrose solution) (kg s^{-1} m^{-3} °C^{-1})
k_{is} rate constant of ice formation on the cooling surface, which is defined as the ice production rate per square meter of cooling surface per degree of supercooling (kg s^{-1} m^{-2} °C^{-1})
L_w thickness of the cooling wall (m)
n rotational speed of the scraper (rpm)
Q heat (kJ)
$r = \sqrt{x^2 + z^2}$ displacement from the origin to the point (x, z) at the X–Z plane (m)
T temperature (K or °C)
T_1 and T_2 temperature in ice and water (Neumann problem) (K or °C)
T_0 water temperature in remote place (Neumann problem) (K or °C)
T_c coolant temperature (a fix temperature in this experiment) (K or °C)
T_f freezing point of aqueous solutions (=−0.6 °C for 10%wt sucrose solution) (°C)
T_l liquid temperature (K or °C)
T_{l0} initial temperature of the liquid (before freezing) (K or °C)
T_s cooling surface temperature (K or °C)
T_{s0} initial temperature of the cooling surface (before freezing) (K or °C)
T_w temperature inside the cooling wall (K or °C)
$\Delta T_s (= T_f - T_s)$ degree of supercooling at the cooling wall surface (K or °C)
$\Delta T_w (= T_f - T_w)$ degree of supercooling of the cooling wall (K or °C)
t time (s)
t_{fit} fouling induction time, which is the time needed for the growing ice to cover the entire cooling surface (s)
V_l and V_w volume of the liquid (or solution) and the cooling wall (m^3)
v growth rate of ice films spreading along the subcooled solid wall (μm s^{-1})
α_1 and α_2 thermal diffusivity ($=\lambda/\rho c$) of ice and water (Neumann problem) (m^2 s^{-1})
α_l and α_w thermal diffusivity of liquid (=1.28 × 10^{-7} for 10%wt sucrose solution) and the solid cooling wall (4.4 × 10^{-6} for stainless steel) (m^2 s^{-1})
δ thickness of the newly formed ice film at the growing front (m)
φ ratio of ice free area to the total area of the scraped surface ($0 \leqslant \varphi \leqslant 1$)
$\kappa = \rho_w c_w / 2\lambda_w$ a constant of the physical property of the cooling wall
λ_1 and λ_2 thermal conductivity of ice and water (Neumann problem), respectively
λ_l and λ_w thermal conductivity of liquid (=0.53 for 10%wt sucrose solution) and cooling wall (=17.45 for stainless steel), respectively (J m^{-1} °C^{-1})
θ angle in the polar coordinate system (rad)
ρ_l, ρ_i, ρ_w density of liquid (=1060 for 10%wt sucrose solution), ice (=917) and solid wall (=7900 for stainless steel), respectively (kg m^{-3})
$\beta = \frac{\Delta H k_s}{\lambda_w}$ represents the contribution of the latent heat transfer of ice formation to the temperature gradient on the scraped-subcooled surface
$\gamma = \frac{\varphi h_l}{\lambda_w}$ Represents the contribution of the sensible heat transfer of the liquid to the temperature gradient on the scraped-subcooled surface
Γ cycle time of the rotating scraper (s)

Subscripts
c, i, l, s, w coolant, ice, liquid (or solution), cooling surface, cooling wall
1 and 2 frozen and thawed region (Neumann problem).

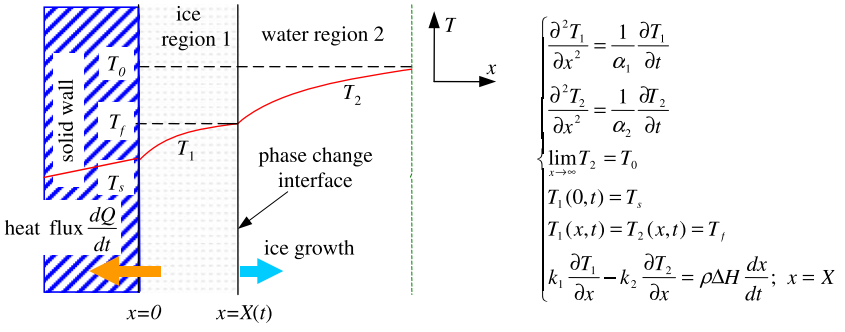

(a) Temperature profile (b) The expression of the Neumann Problem

Fig. 1. The temperature distribution in a partially frozen medium, which is described with the *Neumann problem* presented on the right-hand side.

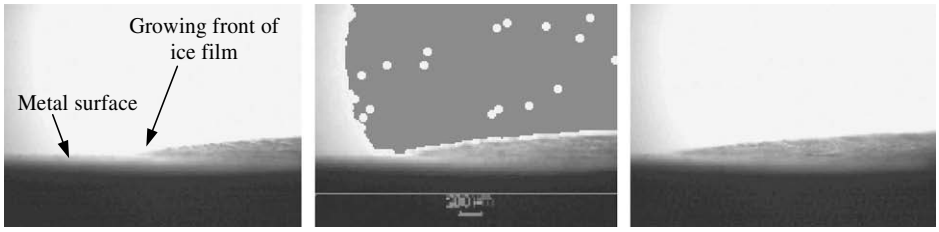

(1) Beginning of freezing (2) at the 10th second (3) at 20th second

Fig. 2. Video pictures of the side view of a growing ice film from a 10%(wt) sucrose solution on a subcooled stainless steel surface with the degree of supercooling of 0.75 °C. The thickness of the ice film is about 250 μm. (1) Beginning of freezing (2) at the 10th second (3) at 20th second.

(1) Beginning of freezing (2) at the 5th second (3) at the 6th second

Fig. 3. Video pictures of the side view of a growing ice film from a 10%(wt) sucrose solution on a subcooled stainless steel surface with the degree of supercooling of 2 °C. (1) Beginning of freezing (2) at the 5it th second (3) at the 6th second.

growing ice films on a subcooled stainless steel surface at different degrees of supercooling. More details can be found in the cited articles above.

The degree of supercooling on the stainless steel cooling surface was about 2 °C in Fig. 3, but it was only 0.75 °C in Fig. 2. The former showed a much faster growth rate, where the ice layer burst out and completely covered the cooling surface within seconds. During this time the upward dendritic growth of ice followed the spreading front of the ice film, as shown in Fig. 3 and Eqs. (2)–(4).

Another phenomenon found in the previous experiment showed that the heat flux across the cooling surface at this moment steeply increased by a factor of at least three. However, after this initial period the ice films started to grow thicker and foul the cooling surface, causing the heat transfer efficiency to decline rapidly [5,19].

Therefore on a subcooled, scraped surface that is submerged in iced water or aqueous solutions, a physical model is proposed using the following analogy: the growth of the ice patches in microscopic scale is somewhat like a macroscopic phenomenon of raindrops hitting the windscreen of a car, i.e. ice nuclei appear on the surface randomly, and then grow as patches along the solid surface transversely. The scraper wipes off the ice from the cooling surface before it covers the whole cooling surface. After the scraper passes over, another round of nucleation and crystallization of ice restarts. This is illustrated in the schematic diagrams of Fig. 4.

1.3. Four problems

Consequently from an engineering point of view, the above-mentioned observation and physical model raise four problems regarding the ice growth on a subcooled solid surface:

Problem 1. How long does it take for the growing ice patches to cover the entire submerged cooling surface?
Problem 2. How can the transient thermal response, which results from the latent heat liberation at the onset of freezing on the cooling plate and in the bulk solutions, be described?
Problem 3. How can the heat transfer at the onset of freezing, which is characterized by a steep increase in heat flux, be described in a comprehensive mathematical way?
Problem 4. How fast is the growing front of the ice layer spreading along the subcooled solid surface?

This paper will present fundamental research in order to answer the above questions. Most of the experiments mentioned in this paper used 10%(wt) sucrose solution as a simulative food liquid, which had a freezing point of −0.6 °C. Otherwise it will be stated if another food liquid, e.g. milk, was used. This is because for most fruit juices and liquid food, such as orange juice, apple juice, sugarcane juice and grape juice, solute concentrations are usually around 8–18%(wt), and the cow milk is around 10%wt as

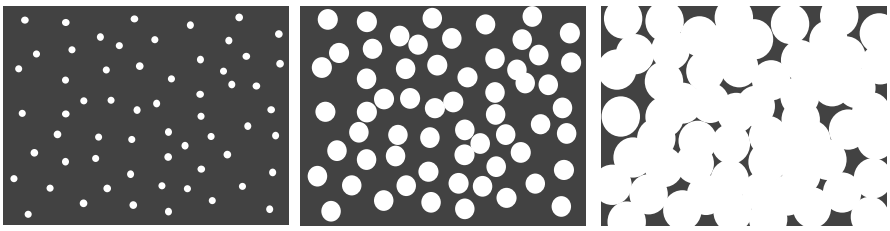

t_1 t_2 t_3

Fig. 4. A proposed physical model of ice nucleation and growth on the subcooled metal surface, where the white area represents ice patches and the black area represents the metal surface.

well. Moreover, sugars (including sucrose, fructose, glucose, lactose, etc.) are the main components that contribute to the freezing point depression of these solutions. The material of the cooling surface is stainless steel, from which most of the food processing machinery including various SSHE(s) are constructed.

2. Mathematical models

2.1. Induction time of ice fouling

The above-mentioned problem 1 can be expressed as the induction time of ice fouling on sub-cooled solid surfaces. When the supercooled liquid (aqueous solution) starts to freeze (nucleation), the liberation of latent heat increases both the cooling surface and bulk solution temperatures steeply. In this study, the steep increase of surface temperature, which was probed with a ϕ0.25-mm T-type thermocouple, was used to indicate the moment of freezing onset. This is shown in Fig. 5, where the onset of ice nucleation was at the 1400th second when both the bulk and surface temperatures jumped. Details of this experiment is available in our previous publication [20].

The ice layer on the cooling surface grew further and eventually covered the entire submersed cooling surface, while the electric impedance increased as well. This was used to indicate the induction time of ice fouling in this study, because the AC current signal vanished when ice covered the entire metal surface. The detector circuit shown in Fig. 6 was built for this purpose. It was the same with the circuit described in the above cited Ref. [20]. Linear regression of the experimental data generated an empirical expression, which correlated the degree of supercooling (ΔT_s) and the mass fraction of ice seed (C_{seed}) with the induction time of ice fouling (t_{fit}).

$$t_{fit} \approx \frac{1}{5.9(C_{seed})^{0.5}\cdot(\Delta T_s)^{2.3}} \tag{1}$$

The symbols in Eq. (1) are explained in nomenclature. Eq. (1) shows that the induction time of ice fouling, which is the time scale for ice films to cover the entire cooling surface, is very sensitive to the degree of supercooling. In a SSHE used for making ice slurry, the time interval between two scraping actions can be estimated from the induction time of ice fouling (see Section 3).

2.2. Thermal response of the onset of nucleation

When ice appears, the liquid temperature increases quickly from the supercooled state until it reaches a quasi steady-state as shown in Fig. 5. The above-mentioned problem 2 can also be interpreted as the thermal response of the system at the onset of

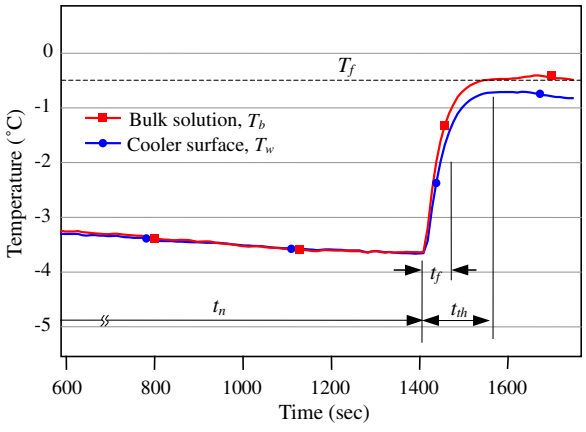

Fig. 5. Temperature tracks of the spontaneous nucleation of ice from whole milk.

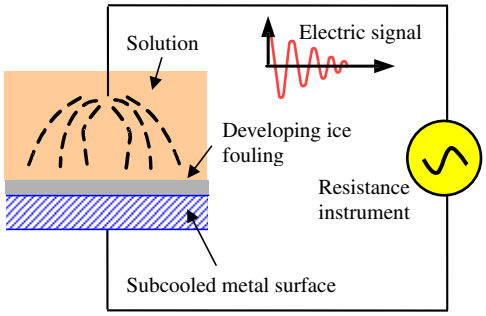

Fig. 6. Coverage of ice fouling on the subcooled surface indicated by the decline of the electrical conductive signal.

freezing [21–25]. In this transient, latent heat of freezing is released and transferred across the metal wall into the cooling media on the other side. There are two equalities that can be found in the bulk solution and in the cooling wall:

Equality I: Heat accumulation in the bulk liquid = latent heat of ice formation – heat transferred to the steel plate and
Equality II: Heat accumulation in the steel slab of the cooling wall = heat transferred into the steel from the bulk – heat transferred out of the steel into the coolant.

Therefore, the following simultaneous differential Eqs. (2) and (3), together with the initial conditions of Eq. (4), are established:

$$c_l V_l \rho_l \cdot \frac{dT_l}{dt} = \Delta H \cdot k_{il} \cdot V_l \cdot (T_f - T_l) - h_l \cdot A_s \cdot (T_l - T_s) \tag{2}$$

$$\frac{c_w V_w \rho_w}{2} \cdot \frac{dT_s}{dt} = h_l \cdot A_s \cdot (T_l - T_s) - \frac{\lambda_w}{L_w} \cdot A_s \cdot (T_s - T_c) \tag{3}$$

$$T_s|_{t=0} = T_{s0}, T_l|_{t=0} = T_{l0} \tag{4}$$

Definitions and the significance of the symbols used in these equations are listed in nomenclature. Eq. (2) is the result of equality I in liquid phase, and Eq. (3) is the result of equality II in the solid cooling wall. Eq. (2) can be resolved by using the Laplace transform and the analytical solution is expressed with Eq. (5). More mathematical and experimental details can be found in Ref. [26].

$$\frac{T_l - T_{l0}}{T_f - T_{l0}} = 1 - \exp\left(-\frac{\Delta H k_{il}}{c_l \rho_l} \cdot t\right) \tag{5}$$

In this article, the same math treatment to the Eq. (3) leads to another analytical solution regarding the cooling surface:

$$\frac{T_s - T_{s0}}{T_f - T_{s0}} = 1 - \exp\left(-\frac{\Delta H k_{il}}{c_l \rho_l} \cdot t\right) \tag{6}$$

This is to say the thermal responses in liquid and on the cooling surface are both expressed in the form of the first-order reaction. The rate constant (k_{il}) of ice formation in the bulk liquid was measured in experiment to be 0.384 kg s^{-1} m^{-3} °C^{-1} [26].

In the liquid phase, the thermal response predicted by Eq. (5) met the experimental results extremely well. However, on cooling surface the thermal response predicted by Eq. (6) had a problem: the experimental value was initially higher than that of the model prediction, but dropped below the model prediction (in ~30 s) and declined further as shown in Fig. 7.

This discrepancy presumably resulted from an assumption when establishing the Eqs. (2)–(4) that ice evenly appears, distributes and exists in the liquid phase and on the subcooled surface all the time. As revealed in problem 1, this assumption may not be true. Once the nucleation starts, ice would grow into a fouling layer even though strong bulk agitation is applied, i.e. ice will stick and

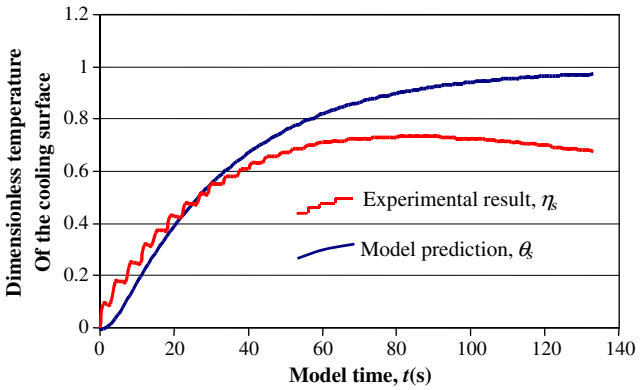

Fig. 7. Comparison of the thermal response of experimental result and model prediction when scraping was not applied to the cooling surface.

accumulate on the cooling surface. Therefore, our explanation for this discrepancy is that the fast growth of ice on the subcooled surface directly released the latent heat of freezing to increase the surface temperature resulting in a quicker temperature rising rate than the model prediction. When the fouling layer is built up subsequently, however, it increased the heat transfer resistance, causing the cooling surface temperature to decline.

Based on this understanding, we applied a rotational scraper (>30 rpm, 2 blades) acting on the cooling surface to prevent ice fouling, and found that the model prediction for the thermal response on the cooling surface given by Eq. (6) met the experimental results very well this time (Fig. 8).

Now that the model predictions for the bulk liquid and cooling surface both meet the experimental results, it is interesting to find that the right-hand of Eqs. (5) and (6) are identical, meaning that the thermal response tracks (T vs t) in the liquid and on the cooling surface have the same form. This can be interpreted that (1) in a supercooled solution in a vessel with cooing jacket, the release of the latent heat of freezing overwhelmingly dominates the thermal response for both the liquid and the cooling surface and (2) if the liquid is well agitated and the cooling surface is scraped to remove ice fouling, the direct contact of the liquid and cooling surface results in an identical thermal response. However the thermal properties and thickness of the cooling wall do not influence the process.

This clarifies some of the confusion in using a cooling jacket in a vessel for freeze concentration of aqueous solutions without scraping the cooling surface [27–31]. The work of this section and the previous section also convinces us that if the degree of supercooling at the cooling wall (i.e. the differential temperature between the freezing point of the solution and the cooling wall) is greater than 0.2 °C, then ice fouling is unavoidable on the unscraped-subcooled bare metal surface. To make ice continuously with a desired efficiency, scraping must be applied to remove the ice from the cooling surface.

2.3. Heat transfer on the subcooled-scraped surface with/without phase change

Numerous studies on heat transfer regarding phase changes have been done in history. Our previous experimental results showed that (1) at the onset of freezing there is a steep increase in the heat flux across the cooling surface; (2) if the fouling ice is removed continuously by scraping the cooling surface, a much higher heat transfer coefficient is obtained than if there is no phase change [5]. Modeling study for this problem has brought up an analytical solution, which is expressed as a step function of the heat transfer coefficient with/without phase change, as briefly narrated below. More details can be found in Ref. [19].

The heat transfer on a scraped surface before freezing (without phase change) can be described in the same way as a diffusion process, and the deferential element (dx) for analyzing and establishing the PDE is taken in the solution as shown in Fig. 9. The problem is defined by the simultaneous Eqs. (7)–(10), where Eq. (7) is the governing differential equation; Eq. (8) is the initial condition and Eqs. (9) and (10) are the boundary conditions. Details of resolving this problem can be found in Ref. [32].

$$\frac{\partial T}{\partial t} = \alpha_l \frac{\partial^2 T}{\partial x^2} \tag{7}$$

$$T(x,0) = T_l \tag{8}$$

$$T(0,t) = T_s \tag{9}$$

$$T(\infty,t) = T_l \tag{10}$$

After freezing starts, however, patches of ice occur on the cooling surface. The new phase (ice) directly releases the latent heat (Q_i) into the cooling surface as a heat source. Meanwhile on the ice-free area the liquid phase transfers the sensible heat (Q_l) to the cooling surface as another heat source. The differential element (dx) for analyzing and establishing the PDE is taken inside the cooling wall, as shown by Fig. 10. The heat transfer problem in this time can be defined by Eqs. (11)–(13), where Eq. (11) is the governing equation, which takes the form of Laplace equation, because there is no heat source inside the cooling wall, and the heat transfer across the metal plate is a quasi steady-state when scraping is applied, resulting in $\frac{\partial T}{\partial t} = 0$. Eqs. (12) and (13) are the boundary conditions.

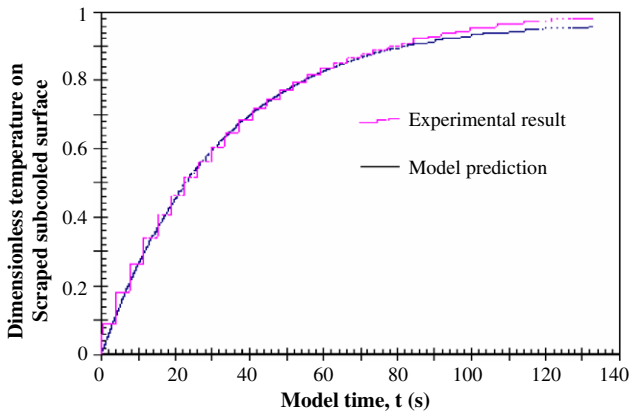

Fig. 8. Comparison of the thermal response of experimental result and model prediction when scraping was applied on the cooling surface.

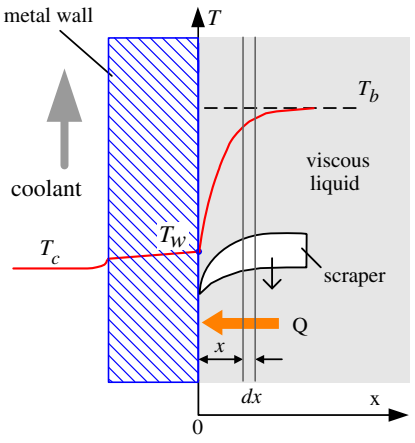

Fig. 9. Heat transfer above the scraped cooling surface before freezing.

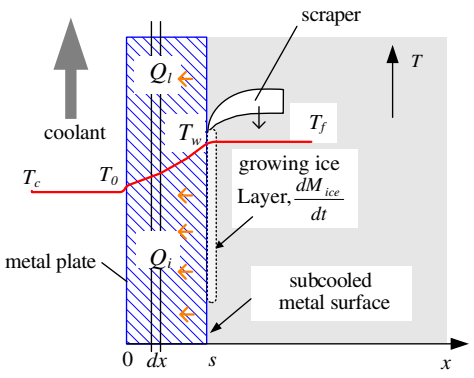

Fig. 10. Heat transfer in the metal plate after freezing.

$$\frac{\partial^2 T}{\partial x^2} = 0 \tag{11}$$

$$T|_{x=0} = T_c \tag{12}$$

$$\left.\frac{\partial T}{\partial x}\right|_{x=s} = (\beta + \gamma)\Delta T_s \tag{13}$$

At right-hand side of Eq. (13), $\beta\Delta T_s$ represents the contribution of the latent heat transfer of ice formation to the heat flux on the cooling surface, $\gamma\Delta T_s$ represents the contribution of the sensible heat transfer of liquid to the heat flux on the cooling surface. More details can be found in Ref. [19]

For the problem without phase change, i.e. Eqs. (7)–(10), an analytical solution can be obtained, which leads to a result for the individual heat transfer coefficient on the cooling surface, as expressed by Eq. (14). For the problem with phase change, i.e. Eqs. (11)–(13), another analytical solution can be worked out, which likewise gives another individual heat transfer coefficient, as expressed by Eq. (14).

$$h = \left(\frac{\lambda_l \rho_l c_l nF}{15\pi}\right)^{1/2}, \quad \text{(without phase change)} \tag{14}$$

$$h = k_{is}\Delta H + \varphi\left(\frac{\lambda_l \rho_l c_l nF}{15\pi}\right)^{1/2}, \quad \text{(with phase change)} \tag{15}$$

Therefore the individual heat transfer coefficient on a subcooled scraped solid surface with or without phase change can be comprehensively expressed by the above equations. The first term ($k_{is}\Delta H$) on the right-hand side of Eq. (15) represents the contribution of the growing ice on the subcooled surface that boosts the heat flux, though the rate constant (k_{is}) of ice formation on the cooling surface remains unknown. The proportional coefficient (φ) in the second term ranges from 0 to 1 ($0 \leqslant \varphi \leqslant 1$), which represents the ratio of the ice-free area on the cooling surface. If there is no phase change occurring, i.e. φ is 1 and k_{is} is 0, the heat transfer coefficient retrieves to Eqs. (14) and (15). Unlike many other heat transfer coefficient expressions found in unscraped surface heat exchangers, the above expressions do not contain the physical properties of the cooling wall material, such as the thermal conductivity, thermal capacity and density. We will find in the next section of this paper that all those physical properties appear in the expression of the growth kinetics equation of the ice film.

Since the expression of the individual heat transfer coefficient (h) has the form of a step function, it predicts a steep increase of heat transfer in a SSHE at the onset of freezing. This was what we found in the experiment as shown in Fig. 11, where a 10%wt sucrose solution was used as a simulative liquid food for the experiment of freeze concentration, although we were not able to measure the value of k_{is} yet in this work. For more details please refer to Ref. [5,33].

These address problem 3 as raised in the Introduction. Note in this case the phase change occurs only on one side of the cooling wall (from the aqueous solution), on the other side of the cooling wall, the (secondary) coolant remained homogeneous. So the heat transfer on this side becomes restrictive for the overall heat transfer coefficient.

2.4. Growth kinetics of ice films

Eq. (15) involves an unknown constant k_{is} which represents the ice production rate per square meter per degree of supercooling of the cooling surface. This constant can be correlated to the properties of the cooling surface material. Doing so will address problem 4 mentioned at the end of the Introduction.

The growing ice appears as thin films. The initial layer was found to be less than 200 μm in experimental observation. The propagation of the ice film proves to be a heat transfer driven growth, i.e. the heat dissipates into the cooling wall from the grow-

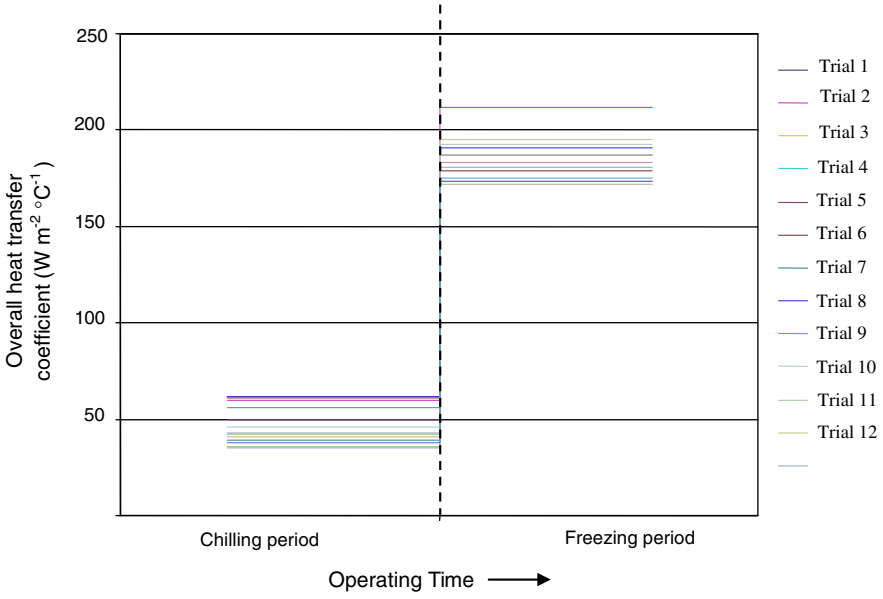

Fig. 11. Experimental results of the step-increase of heat transfer after freezing start.

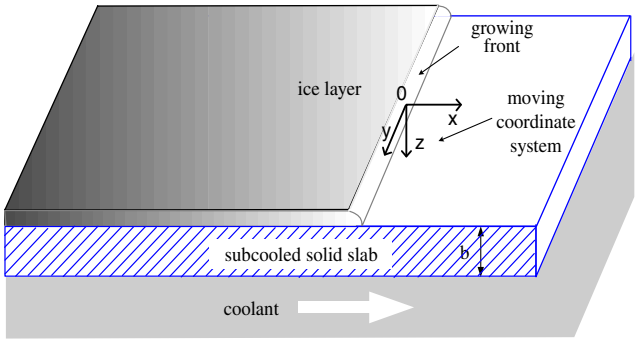

Fig. 12. A schematic diagram of the ice film spreading on subcooled solid surface.

ing front of ice control the spreading speed of ice. To facilitate the mathematical analysis, a moving Cartesian coordinate system that follows the movement of the growing ice front is established with the origin of the coordinate at the heat source, i.e. the growing edge, as shown in Fig. 12. In this coordinate system, the ice front becomes stationary, but the subcooled solid slab is moving in the opposite (negative) direction, as shown in Fig. 13.

In the steady state of film growth, the latent heat of freezing at the growing front equals the heat that is dissipating into the cooling wall at the heat-affected zone (HAZ) underneath the growing front: outside of this small zone the temperature is still the wall temperature, T_w, which is supposed to be a constant for facilitating the analysis. Right below the origin (growing front), the temperature is the freezing point, T_f, of the solution, which is a constant as well. For this problem, the energy equation in the solid slab can be written as Eq. (16) [34]. The boundary condition is given by Eqs. (17) and (18).

$$-v\frac{\partial T}{\partial x}=\alpha_w\left(\frac{\partial^2 T}{\partial x^2}+\frac{\partial^2 T}{\partial z^2}\right) \tag{16}$$

$$T|_{\sqrt{x^2+z^2}\to\infty}=T_w \tag{17}$$

$$T|_{\sqrt{x^2+z^2}\to\delta \text{ and } \theta=\pi/2}=T_f \tag{18}$$

An analytical solution was found as shown in Eq. (19), which includes the Modified Bessel Function in the expression. It describes the temperature distribution in the cooling wall in the region underneath the growing front as illustrated in Fig. 14. More details can be found in Ref. [18].

$$T=T_w+\frac{\Delta T_w}{K_0(\kappa v\delta)}K_0(\kappa v r)\cdot\exp(-\kappa v x) \tag{19}$$

In a very short time period (dt), suppose that the ice film has a growth gain (dl), as shown by Fig. 13. The fusion heat released by

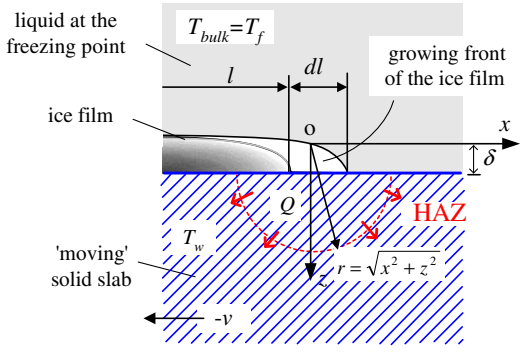

Fig. 13. The cross sectional view of heat transfer from the newly formed ice bud (the white part) into the subcooled solid wall.

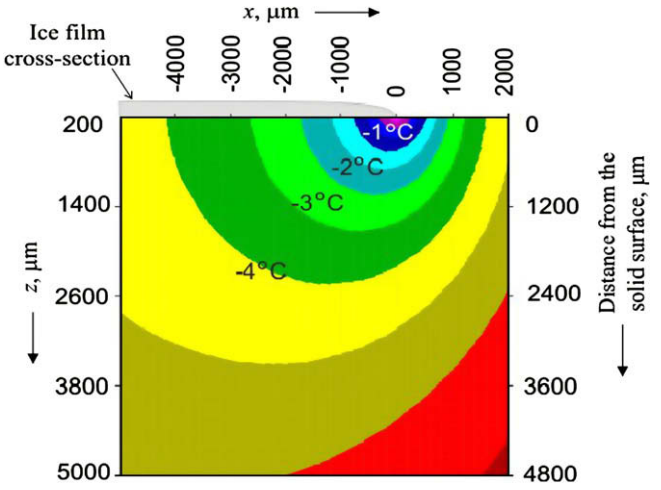

Fig. 14. The temperature distribution in the HAZ of a stainless steel cooling wall at the supercooling of $\Delta T = 5$ °C.

the ice bud can be written as $Q=(dl)\delta\rho_i\Delta H$. Because the ice growth is driven by the heat transfer, the fusion heat must dissipate from the growing front into the solid slab. According to *Fourier's* law, this amount of heat can be expressed as the following double integral surrounding the HAZ which is illustrated in Fig. 13:

$$(\mathrm{d}l)\delta\rho_i\Delta H=\left[\oint_{\mathrm{HAZ}}\lambda_w\left(-\frac{\partial T}{\partial r}\right)ds\right]\cdot(\mathrm{d}t)=-\lambda_w\left[\int_0^{\pi}\left(r\frac{\partial T}{\partial r}\right)_{r=\delta}\mathrm{d}\theta\right]\cdot(\mathrm{d}t) \tag{20}$$

The 'spreading' velocity of the ice film (v) is the ratio of the growth gain (dl) and the time period (dt). Re-arranging Eq. (20) yields:

$$v=\frac{\mathrm{d}l}{\mathrm{d}t}-\frac{\lambda_w}{\rho_i\Delta H}\int_0^{\pi}\left(\frac{\partial T}{\partial r}\right)_{r=\delta}\mathrm{d}\theta \tag{21}$$

After integration, the linear growth rate (v) is given in Eq. (22), in which the growth rate is still in the argument of the modified Bessel functions.

$$\frac{K_1(\kappa v\delta)\cdot I_0(-\kappa v\delta)}{K_0(\kappa v\delta)}+I_1(-\kappa v\delta)-\frac{\rho_i\Delta H}{\pi\lambda_w\kappa\Delta T_w}=0 \tag{22}$$

Eq. (22) is actually the growth kinetic equation of the ice film though the growth rate is expressed with the implicit function. Because for a given solid material (thus λ_w and $\kappa=\rho_w c_w/2\lambda_w$ are fixed) with a given supercooling condition on the surface (ΔT_w, δ), the ice film growth rate (v) is determined. Moreover, the individual heat transfer coefficient is also influenced.

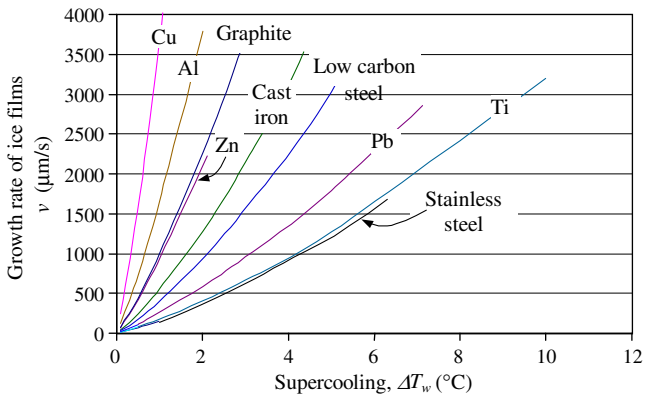

Fig. 15. The growth rate (v) of ice films vs the supercooling (ΔT_w) on metal surfaces.

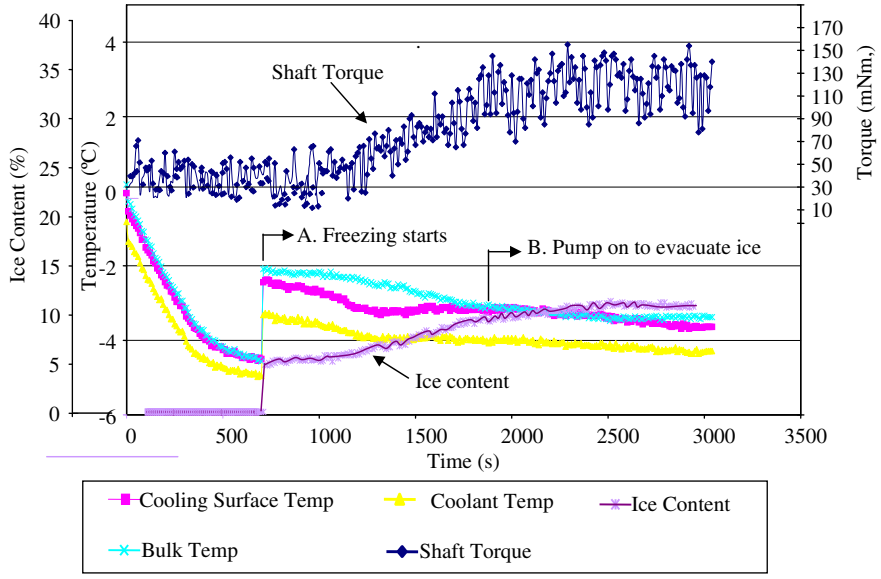

Fig. 16. The process parameters (shaft torque, ice content, temperatures of the cooling surface, the bulk solution and the coolant) vary in a continuously scraped surface heat exchanger. A 5%(wt) ethanol aqueous solution was used in this experiment. The rotational speed was 250 rpm [18].

Fig. 15 shows the ice film spreading velocity on different metal surfaces predicted by Eq. (22). Since Modified Bessel Functions are involved, to obtain these v-vs-ΔT_w curves, a computational method, such as the Mathwork Matlab® or MS Excel® advanced Add-Ins function of Analysis *ToolPak* and *Solver*, can be used for this purpose.

3. Applications and conclusion of the modeling studies

As ice fouling on the cooling surface is unavoidable once freezing starts in a liquid food or an aqueous solution, scraping must be applied to remove the ice in order to produce ice slurry continuously which consequently concentrates the unfrozen solutions. The induction time of ice fouling (t_{fit}) is correlated with the degree of supercooling of the cooling wall, i.e. $t_{fit} \propto 1/(\Delta T)^{2.3}$. This can be used to estimate the 'critical' time interval between two scraping actions. If it is longer than this time, the spreading ice would have covered the entire cooling surface and reduced the heat transfer efficiency. On the other hand, too frequent scraping will consume unnecessary energy. A calculation can be given as follows.

Assuming that the ice is continuously removed from the cooling surface and evacuated from the vessel of the SSHE, so that the ice, which works as seeds to trigger the nucleation, on the cooling surface has a low content, e.g. C_{seed} = 0.01 kg in 1 kg solution, and the supercooling degree of the solution is 2 °C, then the fouling induction time of ice, t_{fit}, according to Eq. (1), is about 0.35 s. If a 4-blade scraper is used, its cycle time is $\Gamma = 4t_{fit}$, i.e. 1.4 s. Thus the rotational speed of the scraper is estimated to be 43 rpm.

At the onset of freezing, phase change directly releases the latent heat to the cooling surface resulting in the heat flux undergoing a steep increase. In this study the phase change occurred only on the side of the solution, but the cooling media in the cooling jacket, which was a secondary coolant, remained in homogeneous. It is foreseeable that if the refrigeration is designed and constructed using the primary coolant in the above cooling jacket, then phase change would occur on both sides of the cooling wall: ice is formed on the side of the solution (and is then scraped off), boiling occur on the other side in the jacket, which also gives a high heat transfer efficiency. Thus the overall heat transfer coefficient would be even higher with a more compact configuration.

As predicted by the model that ice films (in patches) appear on the cooling surface when freezing starts, we presumed that these thin films might be lubricating the scraping action of the scraper on the cooling surface as skating on smooth ice. Experiments were conducted and the shaft torque was measured in order the obtain evidence. This work was published in another article [33]. The experiments did show that the shaft torque reached an even lower value rather than a higher one after the onset of freezing in a SSHE, as shown in Fig. 16 at point A. The shaft torque gradually increased as the ice content accumulated. But the shaft torque could be maintained at a low level to save energy if the produced ice was evacuated continuously as shown in Fig. 16 at point B.

It was interesting to compare this result with others'. Because it was reported that the scraper subjected a sudden resistance increase when freezing started on the cooling surface[15,16]. The main reason may attribute to the difference of the scraping frequency on the cooling surface. We applied relatively higher scraping frequency aiming to remove the ice before it cover the entire cooling surface. However, if the ice slush is built up and covers the entire cooling surface before the next scraping action pass over, the thin film of ice would not be a lubricating factor.

References

[1] V.J. Lunardini, Heat Transfer with Freezing and Thawing, Elsevier Science Pub. Co., Amsterdam/New York, 1991.
[2] S. Haq, J. Harnett, A. Hodgson, Growth of thin crystalline ice films on Pt(III), Surf. Sci. 505 (2002) 171–182.
[3] T. Marshall, C. Girard, Modeling of ice formation and condensation on a cryogenic surface, Fusion Eng. Des. 54 (2001) 473–483.
[4] V.P. Zhdanov, P.R. Norton, Growth of amorphous films at low temperatures: the ice model, Surf. Sci. 449 (2000) L228–L234.
[5] F.G.F. Qin, X.D. Chen, S. Ramachandra, K. Free, Heat transfer and power consumption in a scraped-surface heat exchanger while freezing aqueous solutions, Separ. Purif. Technol. 48 (2006) 150–158.
[6] Anon, Freeze concentration opens new product opportunities, Food Eng., 63 (1993) 50–52.
[7] P. Chen, Freeze Concentration of Food Liquids Using Layer Crystallizers, Ph.D. The University of Auckland. Auckland, New Zealand, 1999.
[8] C.J. Martel, S. Taylor, S.W. Maloney, Freeze Concentration of Pinkwater, Technical Report ERDC TR-02-1, US Army Corps of Engineers, Engineer Research and Development Center, Cold Regions Research & Engineering Laboratory, CRREL Technical Publications, January 2002, p. 19.
[9] W. Gao, D.W. Smith, D.C. Sego, Ice nucleation in industrial wastewater, Cold Regions Sci. Technol. 29 (1999) 121–133.

[10] A.M.H. Debruyn, J.B. Rasmussen, Freeze concentration of ambient waters for toxicity testing, Envir. Toxicol. Chem. 20 (2001) 1733–1739.
[11] S. Holt, The role of freeze concentration in waste, Filtr. Separat. 36 (1999) 34–35.
[12] A. Saito, Recent advances in research on cold thermal energy storage, Int. J. Refrig. 25 (2002) 177–189.
[13] P. Pronk, T.M. Hansen, C.A.I. Ferreira, G.J. Witkamp, Time-dependent behavior of different ice slurries during storage, Int. J. Refrig. 28 (2005) 27–36.
[14] M. Ishikawa, T. Hirata, T. Fujii, Force estimation of mechanical removing processes of mushy structure in an aqueous solution, Int. J. Refrig. 25 (2002) 208–217.
[15] R.J.C. Vaessen, C. Himawan, G.J. Witkamp, Scale formation of ice from electrolyte solutions on a scraped surface heat exchanger plate, J. Cryst. Growth 237–239 (2002) 2172–2177.
[16] Y. Yamazaki, H. Yazawa, Y. Hirata, Hardness of ice layer formed on the wall of a scraped surface crystallizer, Kagaku Kogaku Ronbunshu 24 (1998) 385–391.
[17] M. Ben Lakhdar, R. Cerecero, G. Alvarez, J. Guilpart, D. Flick, A. Lallemand, Heat transfer with freezing in a scraped surface heat exchanger, Appl. Therm. Eng. 25 (2005) 45–60.
[18] F.G.F. Qin, X.D. Chen, M.M. Farid, Growth kinetics of ice films spreading on a subcooled solid surface, Separat. Purif. Technol. 39 (2004) 109–121.
[19] F.G.F. Qin, X.D. Chen, A.B. Russell, Heat transfer at the subcooled-scraped surface with/without phase change, AIChE J. 49 (2003) 1947–1955.
[20] F.G.F. Qin, A.B. Russell, X.D. Chen, L. Robertson, Ice fouling on a subcooled metal surface examined by thermo-response and electrical conductivity, J. Food Eng. 59 (2003) 421–429.
[21] S.G. Kane, Secondary Nucleation of Ice in a Stirred Batch Crystallizer, Sc.D. Thesis. Mass. Inst. Technol., Cambridge, 1971.
[22] Y. Shirai, K. Nakanishi, R. Matsuno, T. Kamikubo, On the kinetics of ice crystallization in batch crystallizers, AIChE J. 31 (1985) 676–682.
[23] J.H. Stocking, C.J. King, Secondary nucleation of ice in sugar solutions and fruit juices, AIChE J. 22 (1976) 131–140.
[24] A.M. Omran, C.J. King, Kinetics of ice crystallization in sugar solution and fruit juices, AIChE J. 20 (1974) 795–802.
[25] D.W. James, R.F. Sekerka, The effect of impurities on solidification kinetics measured by the thermal wave technique, J. Cryst. Growth 1 (1967) 67–72.
[26] F.G.F. Qin, J.C. Zhao, A.B. Russell, X.D. Chen, J.J. Chen, L. Robertson, Simulation and experiment of the unsteady heat transport in the onset time of nucleation and crystallization of ice from the subcooled solution, Int. J. Heat Mass Transfer 46 (2003) 3221–3231.
[27] L. Bayindirli, M. Ozilgen, S. Ungan, Mathematical analysis of freeze concentration of apple juice, J. Food Eng. 19 (1993) 95–107.
[28] Z. Zhang, R.W. Hartel, A multilayer freezer for freeze concentration of liquid milk, J. Food Eng. 29 (1996) 23–38.
[29] R.W. Hartel, L.A. Espinel, Freeze concentration of skim milk, J. Food Eng. 20 (1993) 101–120.
[30] A. Matsuda, K. Kawasaki, H. Kadota, Freeze concentration with supersonic radiation under constant freezing rate – effect of kind and concentration of solutes, J. Chem. Eng. Jpn. 32 (1999) 569–572.
[31] Y. Shirai, T. Sugimoto, M. Hashimoto, K. Nakanishi, R. Matsuno, Mechanism of ice growth in a batch crystallizer with an external cooler for freeze concentration, Agric. Biol. Chem. 51 (1987) 2359–2366.
[32] W.L. McCabe, J.C. Smith, P. Harriott, Unit Operations of Chemical Engineering, sixth ed., McGraw-Hill, Inc., Boston, 2001.
[33] F.G.F. Qin, X.D. Chen, The shaft torque in a laboratory scraped surface heat exchanger used for making ice slurries, Asia-Pac. J. Chem. Eng. 2 (2007) 618–630.
[34] M.N. Ozisik, Heat Conduction, second ed., John Wiley and Sons, New York, 1993.